under which moiré fringes are observed in the X-ray interferometer with continuous radiation are similar to those obtained by Bonse & te-Kaat (1971) for moiré fringes with monochromatic radiation from an extended source (Shulakov & Aristov, 1976)].

The next paper will be devoted to a detailed analysis of the experimental arrangement on the basis of the spherical-wave approximation of diffraction (Kato, 1961) and to the derivation of the dependence of the observed variations of intensity on the experimental geometry and on the dynamical characteristics of the crystal.

References

ARISTOV, V. V., SHMYTKO, I. M. & SHULAKOV, E. V. (1976*a*). Abs. of Rep. 4th All-Union Conf. Dynamical Effects of the Scattering of X-rays and Electrons, 31 March–2 April, Leningrad, p. 11.

ARISTOV, V. V., SHMYTKO, I. M. & SHULAKOV, E. V. (1976*b*). *Kristallografiya*, **21**, 351–356.

ARISTOV, V. V., SHMYTKO, I. M. & SHULAKOV, E. V. (1977). *Acta Cryst.* A**33**, 418–423.

ARISTOV, V. V. & SHULAKOV, E. V. (1975). *J. Appl. Cryst.* **8**, 445–451.

AUTHIER, A. & SIMON, D. (1968). *Acta Cryst.* A**24**, 517–526.

BATTERMAN, B. W. & PATEL, J. R. (1968). *J. Appl. Phys.* **39**, 1882–1887.

BONSE, U. & TE-KAAT, E. (1971). *Z. Phys.* **243**, 14–45.

FUKAMACHI, T. & HOSOYA, S. (1975). *Acta Cryst.* A**31**, 215–220.

HART, M. & LANG, A. R. (1965). *Acta Cryst.* **19**, 73–77.

HART, M. & MILNE, A. D. (1969). *Acta Cryst.* A**25**, 134–138.

HASHIMOTO, H., KOZAKI, S. & OHKAWA, T. (1965). *Appl. Phys. Lett.* **6**, 16–17.

HATTORI, H., KURIYAMA, H. & KATO, N. (1965). *J. Phys. Soc. Japan*, **20**, 1047–1050.

INDENBOM, V. L. & CHUKHOVSKII, F. N. (1972). *Usp. Fiz. Nauk*. **107**, 229–265.

International Tables for X-ray Crystallography (1962). Vol. III. Birmingham: Kynoch Press.

JAMES, R. W. (1948). *The Optical Principles of the Diffraction of X-Rays*, London: Bell.

KATO, N. (1961). *Acta Cryst.* **14**, 627–636.

KATO, N. (1968). *J. Appl. Phys.* **39**, 2225–2230, 2231–2237.

KATO, N. (1969). *Acta Cryst.* A**25**, 119–128.

KATO, N. & LANG, A. R. (1959). *Acta Cryst.* **12**, 787–794.

KOZAKI, S., OHKAWA, T. & HASHIMOTO, H. (1968). *J. Appl. Phys.* **39**, 3967–3976.

KSHEVETSKII, S. A., MIKHAILYUK, I. M. & OSTAPOVICH, M. V. (1975). *Ukr. Fiz. J.* **20**, 610–615.

PINSKER, Z. G. (1974). *Dynamical Scattering of X-rays in Ideal Crystals*. Moscow: Nauka.

SHULAKOV, E. V. & ARISTOV, V. V. (1976). Abs. Rep. 4th All-Union Conference on Dynamical Effects of the Scattering of X-rays and Electrons. 31 March–2 April, Leningrad, pp. 57–58.

TANEMURA, S. & KATO, N. (1972). *Acta Cryst.* A**28**, 69–80.

WALLER, I. (1926). *Ann. Phys.* **79**, 261–273.

ZACHARIASEN, W. H. (1945). *Theory of X-ray Diffraction in Crystals*. New York: John Wiley.

Acta Cryst. (1977). A**33**, 418–423

Dynamical Contrast of the Topographic Image of a Crystal with Continuous X-ray Radiation. II. A Theoretical Study of the Polychromatic Interference Fringes*

BY V. V. ARISTOV, I. M. SHMYTKO AND E. V. SHULAKOV

Solid State Physics Institute, Academy of Sciences of the USSR, Moskovskaya Oblast, Chernogolovska, 142432, *USSR*

(*Received* 31 *March* 1976; *accepted* 13 *December* 1976)

A theoretical analysis is given of the contrast of the topographic image of a perfect crystal with continuous radiation. Conditions for observation of polychromatic interference fringes in this diffraction scheme are analysed on the basis of Kato's dynamical theory of spherical-wave diffraction. The effect of polarization and azimuthal divergence of X-rays on the contrast of topographs is also discussed.

1. Introduction

In the preceding paper (Part I: Aristov, Shmytko & Shulakov, 1977) we have reported the experimental investigation of the contrast on topographical images obtained for perfect single-crystal Si and Ge wafers in a set-up with a point source of divergent continuous X-ray radiation. It was demonstrated that topographs display polychromatic interference fringes.

In the present paper we apply the dynamical theory of spherical-wave diffraction by perfect crystals (Kato, 1961*a*, *b*) to the analysis of contrast on the topographs of perfect crystals, produced by continuous X-ray radiation. The analysis is restricted to the case of symmetric Laue diffraction by the crystal with zero absorption. This approximation enables one to derive simple expressions for the intensity of diffracted radia-

tion, which prove to be in good agreement with the experimental results.

In the calculations we neglect the diffraction-caused divergence of rays of each wavelength in order to be able to apply Kato's theory of spherical-wave diffraction to the calculations of intensity distribution on a film. This is possible if the increase in size of a wavelength spot on the film associated with the diffraction-caused divergence $\Delta\theta$ is far less than the size of the base of the Borrmann fan (triangle GFH in Fig. 1):

$$(D_2+D_3)\Delta\theta \ll 2t\tan\theta \qquad (1)$$

where θ is usually of the order of 5×10^{-5} rad for perfect crystals, D_2+D_3 is the distance from the exit crystal surface to the film, t is the crystal thickness, θ is Bragg's angle. It should be noted that condition (1) must be satisfied only in order that Kato's theory can be used. The results obtained on the basis of this theory are also valid in the case when the diffraction divergence cannot be neglected. This statement follows from the arguments given below and is confirmed by the experiment.

In the analysis of the experimental arrangement shown in Fig. 2, one must not forget that the crystal is illuminated by a divergent wave from a point source. The divergence of rays results in different changes of intensity on a film in the radial **X** and azimuthal **Y** directions. These changes take place independently of one another and can be analysed separately. First we consider the intensity distribution in the radial direction. For simplicity, we assume that the plane of X-ray diffraction coincides with that of $y=0$.

2. Calculation of intensity distribution along the radial direction

Fig. 1 shows Kato's scheme, clarifying the process of propagation of the monochromatic wave field in a crystal. To apply this scheme to the analysis of diffrac-

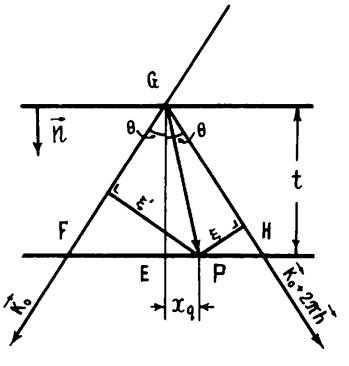

Fig. 1. Scheme clarifying the process of propagation of the monochromatic wave field in a crystal. $\mathbf{K}_0$ and $\mathbf{K}_0+2\pi\mathbf{h}$ are the wave vectors of primary and diffracted waves, P is the observation point on the exit surface of the crystal, the point E is the centre of the base of the Borrmann fan, $|x_q|=EP$.

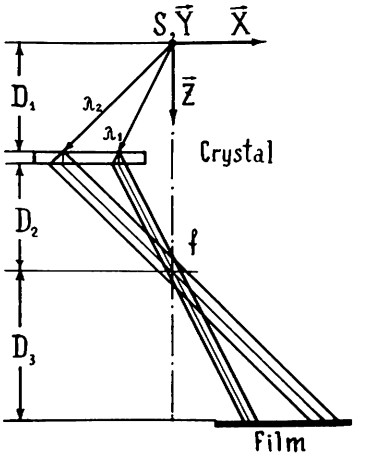

Fig. 2. Scheme of symmetric Laue diffraction of the divergent polychromatic wave on the perfect crystal. D_1 is the distance from the radiation source S to the entrance crystal surface; D_2 is the distance from the exit crystal surface to the focusing point F ($D_1=D_2$); D_3 is the distance from the focusing point to the film ($-D_2\leq D_3<\infty$); **X**, **Y**, **Z** are the Cartesian coordinates with the origin at the point S, the **X** axis is the normal to the reflecting planes, the **Z** axis is the normal to the crystal surface. The directions **X** and **Y** we shall call radial and azimuthal respectively.

tion of polychromatic waves we choose a narrow interval of wavelengths $d\lambda$, such that $d\theta=(d\lambda/\lambda)\tan\theta$ is much smaller than the angular width of the reflexion. The intensity $di_{\mathbf{h}}(x_P)$ of the diffracted wave on the exit surface of the crystal at a point P is determined in this interval $d\lambda$ by the expression derived in Appendix A:

$$di_{\mathbf{h}}(x_P)=(c/256\pi^2)(\cos\theta/KR)\times(KC|\chi_{\mathbf{h}}|/\sin 2\theta)^2\mathscr{J}_0^2(\zeta)\sigma(\lambda)d\lambda\,. \qquad (2)$$

Here c is the light velocity; $K=2\pi/\lambda$; R is the distance from the radiation source S to the observation point P; C is the polarization factor equal to 1 for the σ-polarization and to $|\cos 2\theta|$ for the π-polarization; $\chi_{\mathbf{h}}$ is the **h**th Fourier coefficient of polarizability of the crystal for X-rays of the hkl reflexion; $\mathscr{J}_0(\zeta)$ is Bessel's function of zero order which differs from zero only within the Borrmann fan, *i.e.* when $\zeta^2\geq0$; $\zeta=KC|\chi_{\mathbf{h}}|(\sin 2\theta)^{-1}\times(\xi\xi')^{1/2}$, and the values ξ and ξ' are defined in Fig. 1; $\sigma(\lambda)$ is the spectral density of radiation. In the system of coordinates introduced in Fig. 2, $x_p=-D_1\tan\theta+x_q$ where x_q varies along the **X** axis and is equal to the distance from point E to point P.

We now calculate the intensity $dI_{\mathbf{h}}(x)$ on a film placed at a distance D_2+D_3 from the crystal exit surface. Let condition (1) be satisfied, *i.e.* the divergence of the diffracted beam in the wavelength range $d\lambda$ can be neglected. Then each point P on the crystal surface corresponds to a point x on the film. This point lies at the intersection of a ray, traced from the point P and parallel to the wave vector of the diffracted wave, $\mathbf{K}_0+2\pi\mathbf{h}$, with the film. Because of the parallel transfer of the wave field from the crystal exit surface to the film plane,

the distribution $dI_h(x)$ is a replica of the distribution $di_h(x_p)$, with the coordinates x and x_p related to the experimental geometry and the variable x_q by the condition:

$$x=(D_1+D_3)\tan\theta+x_p=D_3\tan\theta+x_q\,. \qquad (3)$$

Owing to the azimuthal divergence of a diffracted wave the intensity on the film in the wavelength range $d\lambda$ is $m_y=(2D_1+D_3)/D_1$ times less than that on the crystal. Finally we can write

$$dI_h(x)=m_y^{-1}di_h(x_p)\,. \qquad (4)$$

For polychromatic wave diffraction by a crystal, the field intensities with different λ are superposed in each point x of the film. The range of λ values which contribute to the intensity at this point are determined by (3), *i.e.* by the dimensions of the Borrmann fan and the experimental geometry. Let us calculate the intensity of a diffracted wave on the film by substituting the expression for $di_h(x_p)$ into (4) and then integrating the expression obtained over $d\lambda$:

$$I_h(x)=m_y^{-1}(c/256\pi^2)$$
$$\times\int_{\lambda_1}^{\lambda_2}(\cos\theta/KR)\,(KC|\chi_h|/\sin 2\theta)^2\mathscr{J}_0^2(\zeta)\sigma(\lambda)d\lambda\,. \qquad (5)$$

For the calculation of the integral in (5), we express the variable ζ in terms of x and x_q and integrate with respect to dx_q by change of variables. From Fig. 1, (3) and Bragg's equation, $2d_h\sin\theta=\lambda$, it follows that

$$\zeta=2\pi d_h C(|\chi_h|/\lambda^2)[(t/D_3)^2(x-x_q)^2-x_q^2]^{1/2} \qquad (6)$$

$$d\lambda=-(2d_h/D_3)\cos^3\theta dx_q\,. \qquad (7)$$

The condition $\zeta^2\geq 0$ defines the limits of variation of x_q:

$$a=-xt/(D_3-t)\leq x_q\leq xt/(D_3+t)=b\,. \qquad (8)$$

The quantity $x_{q2}=b$ determines the values of the upper limit of integration in (5), and $x_{q1}=a$ determines the lower. We shall assume that

$$D_3\gg t\,. \qquad (9)$$

This assumption fits the experiment well since $t\lesssim 2$ mm and D_3 is normally greater than 5 cm. In this case, a change in all variables, except for Bessel's function, can be neglected within the integration limits determined by inequalities (8). Taking into account the above considerations, the integral in (5) is written in the form:

$$I_h(x)=\left(\frac{c}{256\pi^2}\right)\left(\frac{\cos\theta}{KR}\right)\left(\frac{KC|\chi_h|}{\sin 2\theta}\right)^2\left(\frac{\sigma(x)}{m_x m_y}\right)$$
$$\times\int_a^b\mathscr{J}_0^2[\zeta(x,x_q)]dx_q\,. \qquad (10)$$

Here $m_x=D_3/D_1$ is the image magnification factor in the radial direction **X**, $\sigma(x)=[2d_h\sigma(\lambda)\cos^3\theta]/D_1$ is the linear density of radiation diffracted at the entrance crystal surface at the point $x'=-m_x x$. The values θ, λ and x in (10) are related by Bragg's equation and the equation $x=D_3\tan\theta$. The integral in (10) is calculated in Appendix *B*. By substituting it into (10), we obtain the final expression for $I_h(x)$:

$$I_h(x)=\frac{\pi}{2}T(x)\int_0^{2A}\mathscr{J}_0(\varrho)d\varrho\,. \qquad (11)$$

Here

$$T(x)=(c/128\pi^3)\,(KR)^{-1}$$
$$\times(KC|\chi_h|/\sin 2\theta)[\sigma(x)/m_x m_y] \qquad (11.1)$$

$$2A=KC|\chi_h|t/\cos\theta\,. \qquad (11.2)$$

In terms of the accuracy of m_x^{-1}, m_y^{-1} and $\sigma(x)$, the approximate formula (11) for a polychromatic integral intensity in the case of a transparent crystal takes the same form as that for the integral intensity of transverse patterns in a monochromatic wave (Kato, 1961*b*) or as that for angular integral intensity in the plane-wave theory (Waller, 1926). In the case of an absorbing crystal, or for small distances D_3, the expressions for various integral intensities differ, since in the case under discussion the polychromatic integral intensity is formed by summation at each point of the rays from different distributions di_h. The basic difference between monochromatic $I_{h,mh}$ and polychromatic $I_{h,ph}$ intensities lies in the fact that for obtaining a change in $I_{h,mh}$ the crystal thickness must be varied, while $I_{h,ph}$ varies even in the case of diffraction on a plane-parallel crystal, since the wavelength and hence the parameter A vary in the radial direction.

The maxima of the polychromatic integral intensities are found from the condition $2A=\varrho_{2l+1}$, where $l=0,1,2,\ldots$; ϱ_{2l+1} are zeros of Bessel's function of the zero order. For large l, oscillations are of sinusoidal character with period $\Delta A=\pi$, and the fringe spacing on the film is found from (11.2). The form of the intensity distribution $I_{h,ph}$ depends also on the coefficient $T(x)$ which takes into account the experimental geometry, the spectral composition of radiation used and the position of the observation point x.

In the above consideration we neglected the diffraction-caused divergence. This approximation may not hold for large crystal–film distances and for thin crystals [see equation (1)]. Nevertheless, the obtained result remains valid for this case. The following qualitative arguments allow such a conclusion to be drawn. When the distance D_3 increases, the diameter of the diffraction spot, caused by diffraction of one monochromatic divergent wave, varies only negligibly in the radial direction and is approximately equal to $2t\tan\theta+5\times10^{-5}(D_2+D_3)$, the net intensity of such a spot remaining constant. The distance between the maxima of the integral intensity increases proportionally to D_3 and the interval of summation $\Delta\lambda=\lambda_2-\lambda_1$ at the film point x [see equation (5)] decreases proportionally to D_3. Therefore for very large distances D_3 the intensity at each point x on the film can be assumed equal to

the net intensity of the corresponding diffraction spot, obtained by the diffraction of a monochromatic divergent wave, divided by the coefficient of azimuthal magnification. This means that the distribution of intensity $I_{\mathbf{h},ph}$ is again described by (11).

Note that the oscillations of integral intensity $I_{\mathbf{h},ph}$ for the σ and π polarizations have periods which differ by the coefficient $|\cos 2\theta|$. This can give rise to the deterioration of the contrast of interference fringes of the total intensity. The dependence of the fringe contrast of $I_{\mathbf{h},ph}$ on the polarization in the **Y** direction has been discussed by us in the preceding paper when analyzing the topographic image of a wedge-shaped crystal. This dependence was found to be similar to that for $I_{\mathbf{h},mh}$ investigated by Hattori, Kuriyama & Kato (1965), Hart & Lang (1965) and others. The effect of polarization on the contrast of interference fringes in the **X** direction has no such an analogue, and is discussed in detail in the next section.

3. Effect of polarization of X-rays in the radial direction

The X-ray radiation is not polarized, so that the observed interference pattern contains two oscillations with periods Λ_x^π and Λ_x^σ for the π and σ polarizations respectively. Superposition of two oscillations with closely spaced periods results in the appearance of a period $(\Lambda_x)^{-1}=(\frac{1}{2})[(\Lambda_x^\pi)^{-1}+(\Lambda_x^\sigma)^{-1}]$. The amplitude of these oscillations is modulated by a wave with period $(\Lambda_e)^{-1}=(\frac{1}{2})[(\Lambda_x^\pi)^{-1}-(\Lambda_x^\sigma)^{-1}]$. For Si the value of Λ_x remains approximately constant over a wide range of wavelengths λ. However, the absence of periodicity for the π-polarization gives rise to the fact that the value Λ_e rapidly diminishes and the fringe contrast deteriorates as the wavelength increases. It can be shown that the radiation wavelength λ_e^n, for which n-fold fading of contrast takes place on a topograph because of the superposition of the π and σ waves in opposite phases, is determined by the expression

$$\lambda_e^n \simeq [(2n-1)t_0/t]^{1/3}\lambda_{e0}^1 . \qquad (12)$$

Here t is the crystal thickness, n is the integer, λ_{e0}^1 is the wavelength for which the first fading of contrast is produced on the crystal thickness $t_0=1$ mm, $\lambda_{e0}^1=(d_{\mathbf{h}}^2\lambda^2/|\chi_{\mathbf{h}}|t_0)^{1/3}$. In the case of the 111 reflexion in Si $\lambda_{e0}^1=0{\cdot}662$ Å. The distance between the points of contrast fading rapidly decreases as n rises. As a result, for large n the contrast of interference fringes on a topograph disappears. The number of fringes N between two neighbouring areas of contrast fading is approximately equal (for large n) to

$$N \simeq 2d_{\mathbf{h}}^2/3\lambda^2. \qquad (13)$$

The analysis of (13) shows that in the case of the 111 reflexion in Si the polychromatic integral intensity fringes can be observed practically only up to $\lambda_{\text{bound}} \sim 1{\cdot}3$ Å. For larger wavelengths the ratio Λ_e/Λ_x becomes less than 4 for any thickness t. Note that on thick crystals a greater number of fringes are observed between two areas of fading; *e.g.* 15 fringes are observed on 2 mm thick Si wafer between the first and second fadings, and only three fringes on a 0·2 mm thick wafer.* This means that polychromatic interference fringes appear almost exclusively in the case of diffraction by sufficient thick crystals. Thus, in the experiments described in the first paper the fringes were observed on plane parallel crystals not less than 0·3 mm thick, and the maximum contrast conditions corresponded to $t=1-2$ mm. If t was further increased, the absorption became considerable and interference fringes disappeared. The analysis of (12) and (13) and of the expression for λ_{e0}^1 demonstrates that the conditions for the observation of fringes with the same values of n rapidly deteriorate as indices of planes (hkl), from which reflexions are obtained, increase. Hence, polychromatic integral intensity fringes for the reflexions from high-indices planes can be obtained only in the case when this reflexion is produced by diffraction from a crystal of the short-wave range of the X-ray spectrum. For example, $\lambda_{\text{bound}} \simeq 0{\cdot}78$ Å and $\lambda_{e0}^1 \simeq 0{\cdot}45$ Å for the 220 reflexion of Si, and $\lambda_{\text{bound}} \simeq 0{\cdot}45$ Å, $\lambda_{e0}^1 \simeq 0{\cdot}34$ Å for the 422 reflexion of Si.

The above arguments indicate that the presence of two states of polarization in the radiation incident on the crystal affects drastically the contrast of polychromatic interference fringes. A good contrast can be observed on Si only for the diffraction of radiation with $\lambda<1$ Å, with sufficiently thick crystals ($\mu t \simeq 0{\cdot}5-1{\cdot}5$) and only for the reflexions with low hkl indices.

4. Variation of integral intensity in the azimuthal direction

The foregoing considerations concerned only the case for which the plane of X-ray diffraction (the plane containing the wave vector of the incident wave and a normal to reflecting planes) is perpendicular to the crystal surface. From the experimental geometry it follows that when incident rays deviate from the plane of drawing in Fig. 2 towards the azimuthal direction, the diffraction plane is rotated around a normal to the reflecting planes by an angle φ, calculated by the expression:

$$\tan\varphi = y/(2D_1+D_3). \qquad (14)$$

Here y is the coordinate on the film in the azimuthal direction **Y**. The origin of the coordinates ($y=0$) lies in the plane of drawing in Fig. 2.

We now calculate the intensity of diffracted waves in the azimuthal direction. According to Kato's theory the distribution of intensity on the exit surface of the crystal for a given wavelength depends on the crystal thickness in the diffraction plane. The crystal thickness in different diffraction planes varies as $t/\cos\varphi$ with the angle φ increasing. Hence it follows that the conclu-

* In fact, a smaller number of fringes is observed, since the fringe contrast on the interval ends between two areas of fading is low.

sions reached for the diffraction in the diffraction plane, $\varphi=0$, can be expanded to any diffraction plane making an angle φ with the normal to the crystal surface, if we substitute $t/\cos\varphi$ for t in all the equations.*

For example, in the case of diffraction of the polychromatic wave on the plane-parallel crystal, the lines of constant intensity are determined by the equality $A=$constant. (11.2) and (14) and have the following form:

$$x\left[1+\left(\frac{y}{2D_1+D_3}\right)^2\right]^{1/2}=\text{constant}. \qquad (15)$$

These curves are bent towards shorter wavelengths (to smaller x). At $y\ll(2D_1+D_3)$ this bending is hardly noticeable on topographs, the constant integral intensity lines appear to be straight lines similar to the lines of characteristic radiation.

In order to check the validity of the conclusions of this section we recorded topographs in the experimental arrangement described in the preceding paper from the plane-parallel crystal tilted by different angles φ_0. The angle φ is measured between the normal to the surface and the diffraction plane. Rotation was performed with respect to the axis perpendicular to the reflecting planes. As the angle φ increases, the fringe spacing of integral intensity diminishes by $\cos^{-1}\varphi$ times, which corresponds to the conclusions of the theory. For greater angles φ_0 the topographs also reveal certain tilting of fringes toward smaller values of λ, and the lines of constant integral intensity intersect the lines of characteristic radiation (see Fig. 3). The intensity distribution along the line of characteristic radiation changes as the angle φ varies. For example, the intensity distribution corresponding to the maximum of integral intensity (Part I, Fig. 3*a*) appears for the line Ag $K\alpha$ in the Si 111 reflexion (wafer thickness 0·8 mm, angle $\varphi_0=30°$) after $\Delta\varphi\sim13°$. On the basis of the known experimental geometry, dynamical parameters can be found from the change of contrast on a characteristic line. The change of integral intensity in the azimuthal direction sets in sufficiently slowly and is unnoticeable for angles $\varphi<10°$. The effect of azimuthal divergence must be taken into account in the precise measurements of Λ_x and in the analysis of intensity distributions of characteristic lines.

Conclusions

We have analysed the contrast of topographs obtained with continuous X-ray radiation from a point source of divergent waves. This contrast is produced by superposition of different intensity distributions. The method of summation of these distributions differs from those considered earlier for the case of monochromatic waves, although, if certain conditions are satisfied, they lead to the same results. The observation of polychromatic integral intensity fringes is hindered by the presence in the X-ray radiation of two states of polarization. Contrast fringes can appear only on a limited number of reflexions, obtained in the case of diffraction from a thick crystal of waves with sufficiently small values of λ.

The results obtained may serve as a basis for the development of new methods of measurement of dynamical parameters of crystals over a wide range of wavelengths, and promise new possibilities of studying the diffraction of X-rays by perfect and slightly strained crystals.

APPENDIX *A*

The wave field at a distance r from the point source of polychromatic radiation can be represented in the form of a package of monochromatic spherical waves $E^i(\lambda,r)$:

$$E^i(\lambda,r)=\frac{a^i(\lambda)}{4\pi r}\exp\left[i(Kr-\omega\tau)\right]. \qquad (A.1)$$

Here $a^i(\lambda)$ is Fourier's decomposition component of the ith elementary radiation with respect to monochromatic waves, ω is the cyclic frequency, τ is the time.*

After diffraction by the crystal the wave field E^i is transformed into the fields E^i_0 and $E^i_{\mathbf{h}}$ propagated in the directions of primary and diffracted waves, respectively. According to Kato's (1961*b*) theory, describing the spherical-wave diffraction by a perfect crystal, the intensity of the field $E^i_{\mathbf{h}}$ on the exit crystal surface at the point $\mathbf{r}_p$ is found from the expression:

$$|E^i_{\mathbf{h}}(\lambda,\mathbf{r}_p)|^2=(|a^i(\lambda)|^2/32\pi)\times(\cos\theta/Kr_p)(KC|\chi_{\mathbf{h}}|/\sin 2\theta)^2\mathcal{J}^2_0(\zeta). \qquad (A.2)$$

Averaging the intensity determined by expression (*A*.2) over all radiation for a long period of time, we obtain

$$\frac{c}{8\pi}\langle\sum_i|E^i_{\mathbf{h}}(\lambda,\mathbf{r}_p)|^2\rangle=\left(\frac{c}{256\pi^2}\right)\left(\frac{\cos\theta}{Kr_p}\right)\left(\frac{KC|\chi_{\mathbf{h}}|}{\sin 2\theta}\right)^2\mathcal{J}^2_0(\zeta)\sigma(\lambda) \qquad (A.3)$$

Here $\sigma(\lambda)=\langle\sum_i|a^i(\lambda)|^2\rangle$ is the spectral radiation density, braces $\langle\ldots\rangle$ denote averaging over time.

The intensity $\mathrm{d}i_{\mathbf{h}}(\mathbf{r}_p)$ in the wavelength interval $\mathrm{d}\lambda$ of polychromatic radiation is obtained by multiplication of the right-hand side of expression (*A*.3) by $\mathrm{d}\lambda$.

APPENDIX *B*

By using the notation $a=-tx/(D_3-t)$; $b=tx/(D_3+t)$; $B=2\pi d_{\mathbf{h}}C(|\chi_{\mathbf{h}}|/\lambda^2)(1-t^2/D_3^2)^{1/2}$, we transform the integral in (10) to the form

* The analysis of this problem in terms of the plane-wave theory leads to the same results, *i.e.* for $\varphi\neq0$ the parameter A must be replaced by $A/\cos\varphi$.

* The meanings of the other symbols are explained in the text of the paper.

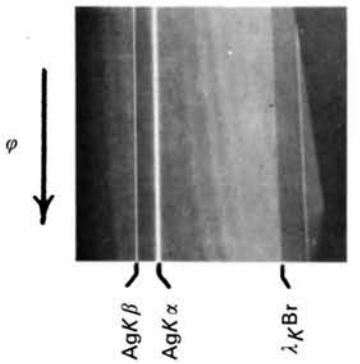

Fig. 3. Topographic image of a plane parallel wafer of Si when the diffraction plane is inclined to the normal of the crystal surface by the angle $\varphi_0 = 30°$. The arrow indicates the direction of an increase in the angle φ.

[*To face p.* 422

$$I=\int_a^b \mathscr{I}_0^2\{B[(x_q-a)(b-x_q)]^{1/2}\}\mathrm{d}x_q . \qquad (B.1)$$

Strictly speaking, the parameter B depends on x_q; however, both the polarization factor C and $|\chi_{\mathbf{h}}|/\lambda^2$ can be assumed constant within the integration limits if condition (9) is satisfied. Assuming $B=$constant, we calculate the integral in expression (*B*.1) following Kato's (1961*b*) method. Let $\mathscr{I}_0^2(\zeta)$ be in the form of a series:

$$\mathscr{I}_0^2(\zeta)=\sum_{m=0}^{\infty}(-1)^m\frac{1}{(m!)^2}\frac{(2m-1)!!}{(2m)!!}\zeta^{2m}. \qquad (B.2)$$

Using decomposition (*B*.2) and having made a change of variables in (*B*.1): $u=(x_q-a)/(b-x_q)$, we have:

$$I=B^{-1}\sum_{m=0}^{\infty}(-1)^m\frac{1}{(m!)^2}\frac{(2m-1)!!}{(2m)!!}[B(b-a)]^{2m+1}\times\int_0^{\infty}\frac{u^m}{(1+u)^{2m+2}}\mathrm{d}u . \qquad (B.3)$$

The integral in (*B*.3) is the tabulated (Dwight, 1961):

$$\int_0^{\infty}\frac{u^m}{(1+u)^{2m+2}}\mathrm{d}u=\frac{(m!)^2}{(2m+1)!}. \qquad (B.4)$$

Substituting (*B*.4) into (*B*.3) we have the expression which can be written:

$$I=B^{-1}\int_0^{B(b-a)}\mathscr{I}_0(\varrho)\mathrm{d}\varrho . \qquad (B.5)$$

Here

$$B(b-a)=(KC|\chi_{\mathbf{h}}|t/\cos\theta)(1-t^2/D_3^2)^{-1/2}=2A(1-t^2/D_3^2)^{-1/2} \qquad (B.6)$$

where A is the parameter of the dynamical theory of X-ray diffraction introduced by Zachariasen (1945). Since we assumed condition (9) to be satisfied, the upper limit of integration in (*B*.5) is equal to $2A$, $B\simeq KC|\chi_{\mathbf{h}}|/2\sin\theta$, and (*B*.5) corresponds to Waller's integral.

References

ARISTOV, V. V., SHMYTKO, I. M. & SHULAKOV, E. V. (1977). *Acta Cryst.* A**33**, 412–418.

DWIGHT, H. B. (1961). *Tables of Integrals and Other Mathematical Data*. New York: Macmillan.

HART, M. & LANG, A. R. (1965). *Acta Cryst.*, **19**, 73–77.

HATTORI, H., KURIYAMA, H. & KATO, N. (1965). *J. Phys. Soc. Japan*, **20**, 1047–1050.

KATO, N. (1961*a*). *Acta Cryst.* **14**, 526–532.

KATO, N. (1961*b*). *Acta Cryst.* **14**, 627–636.

WALLER, I. (1926). *Ann. Phys.* **79**, 261–273.

ZACHARIASEN, W. H. (1945). *Theory of X-ray Diffraction in Crystals*. Sec. III, 8. New York: John Wiley.

Acta Cryst. (1977). A**33**, 423–425

The Use of Structure Factors to find the Origin of an Oriented Molecular Fragment*

BY A. D. RAE

School of Chemistry, University of New South Wales, Kensington, NSW 2033, *Australia*

(*Received* 7 *July* 1976; *accepted* 1 *November* 1976)

When a molecular fragment has a known orientation, it is possible test rapidly all possible positions in the unit cell for this fragment by calculating structure factors at each position for a moderately large number of reflexions. A program, *LOCOFOROM*, has been written for this purpose and application to two structures is discussed.

Introduction

The location of a known molecular fragment in a crystal often takes place in two distinct stages. The first, and usually the easiest, stage is the determination of the orientation of the fragment. Indeed, it has long been recognized that a consistent but incorrect set of phases from a statistical model often yields an E map with recognizable molecular fragments of correct orientation but wrong position.

The orientation of a fragment may often be unambiguously obtained from the Patterson function (Nordman, 1970) or from a comparison of a calculated transform for a fragment with the observed reflexions (Tollin & Cochran, 1964). This information is sometimes used to assist statistical phase-determination methods (Thiessen & Busing, 1974).

The second stage is the determination of the positions in the crystal for these fragments. However, difficulties are often encountered at this stage and the

* Research performed at Oak Ridge National Laboratory and sponsored by the Energy Research and Development under contract with Union Carbide Corporation.